Australian Government
Geoscience Australia

Satellite Radar Interferometry: Application to Rabaul Caldera, Papua New Guinea

David Hutchinson & John Dawson

Record
2009/39
GeoCat
#69305

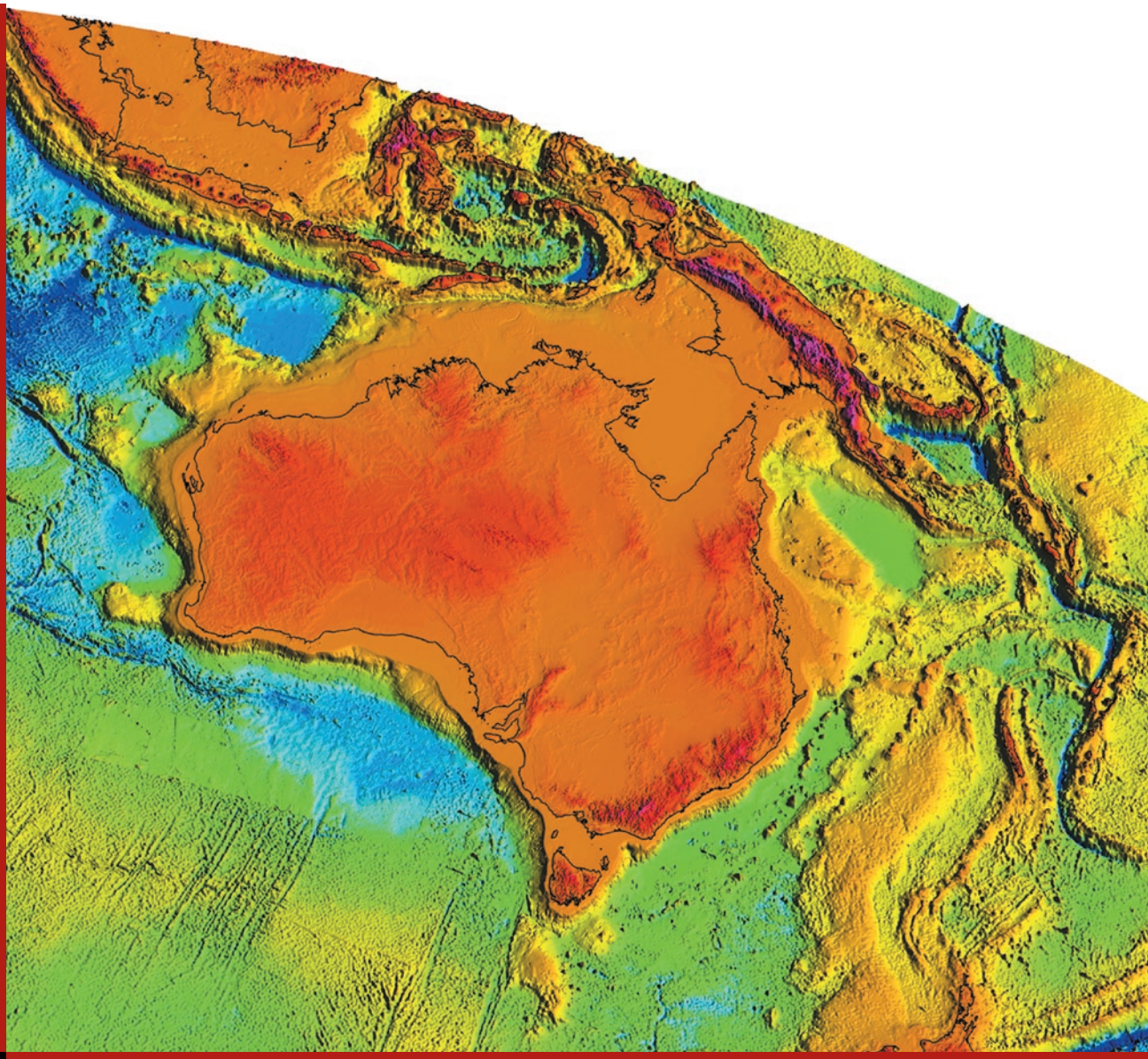

Satellite Radar Interferometry: Application to Rabaul Caldera, Papua New Guinea

GEOSCIENCE AUSTRALIA
RECORD 2009/39

by

David K. Hutchinson [1] and John H. Dawson [1]

1. Geoscience Australia

Department of Resources, Energy and Tourism
Minister for Resources and Energy: The Hon. Martin Ferguson, AM MP
Secretary: Mr John Pierce

Geoscience Australia
Chief Executive Officer: Dr Neil Williams PSM

ISSN 1448-2177
ISBN 978-1-921672-36-1

GeoCat # 69305

Bibliographic reference: Hutchinson, D.K. and Dawson, J.H., 2009, Satellite Radar Interferometry: Application to Rabaul Caldera, Geoscience Australia Record **2009/39**, 19pp**.**

Contents

Executive Summary

Interferometric synthetic aperture radar (InSAR) is a geodetic monitoring tool used to measure ground deformations at centimetre-scale precision. InSAR has been used to study many geophysical phenomena, including volcanoes and earthquakes. This technique has yet to be applied widely in Papua New Guinea, despite its potential as a hazard monitoring tool for the numerous volcanoes in the region. This study applies InSAR to the Rabaul caldera, to investigate the feasibility of the technique in the region. This location was chosen so that the results of this study can be compared to ground based measurements provided by the Rabaul Volcano Observatory.

Of the 10 radar images acquired for this study, 7 were successfully processed to form interferograms. These interferograms were then stacked together to form a time series of deformations, spanning a 14 month period from 27 February 2007 to 16 April 2008. Most of these interferograms had high coherence, and relatively low noise, with centimetre-scale deformations evident in the deformation time series. These results suggest that this technique is capable of detecting surface deformation associated with volcanic eruptions. The primary limitations to the analysis were the availability of radar data, and the baseline separation between acquisitions. We were unable to apply temporal filtering to remove atmospheric noise, since there were too few acquisitions in the time series.

Introduction

RABAUL

Rabaul caldera has had numerous periods of activity during the 20th century. Its activity poses a major danger to local residents, as well as the infrastructure of Rabaul town. The most notable eruption in terms of human cost was the eruption of 1937, which killed 500 people. The last major eruption occurred in 1994, which destroyed much of Rabaul town and its infrastructure. It continues to pose a significant danger to the town and its residents. The ash clouds produced by the volcano are also hazardous for aircraft.

Rabaul Caldera

Rabaul caldera is one of many calderas on the Gazelle Peninsula in the northeast of New Britain. Rabaul caldera contains two active volcanoes, Vulcan and Tavurvur, as well as several other dormant ones. There is a significant magma reservoir located at 3-6 km depth beneath the caldera, as revealed by seismic tomographic imaging (Finlayson et al., 2003). The Rabaul caldera presents an ideal location for testing the InSAR technique in Papua New Guinea (PNG), because it contains active volcanoes, and there are a number of ground based geodetic monitoring stations in the area. The ground based geodetic systems can be used to validate the results found in this study, and to assess the accuracy of InSAR in this region. InSAR may also be able to reveal activity in the region that has not been observed previously, which can assist in choosing where to deploy ground based monitoring systems.

Rabaul Volcanological Observatory (RVO)

Geoscience Australia (GA) and its predecessors have been involved in monitoring the Rabaul volcanic complex since the 1940s. GA has a long term partnership with the Rabaul Volcanological Observatory (RVO), which is responsible for monitoring volcanoes throughout PNG. GA provides scientific and technical assistance to the RVO, through a hazard monitoring programme funded by the Australian Agency for International Development (AusAID). A detailed account of the partnership between GA and the RVO can be found elsewhere (AusAID, 1996; Fisher, 2005).

One of the aims in the partnership between GA and the RVO is to help the RVO become more self-sufficient in their capacity to monitor volcano hazards. However, due to limited resources, it remains advantageous for the RVO to collaborate with agencies in developed countries. Agencies such as GA have the capacity to purchase and process remote sensing data, in situations where the RVO lacks the technology or funding to perform their own analysis. Partnerships like this are likely to remain important to the RVO, especially as remote sensing techniques become more advanced and widespread.

VOLCANO HAZARD MONITORING

Predicting volcanic eruptions is a challenging process, since it usually requires a suite of different monitoring techniques. These techniques consist of both ground based measurements and remote sensing techniques. Ground based measurements consist primarily of seismic monitoring, ground deformation measurements using GPS and tiltmeters, and monitoring of gaseous emissions such as sulphur dioxide. Seismometers and GPS devices provide useful real-time volcano monitoring. However they are expensive to set up and maintain, and therefore are usually available only in a few

selected locations. Thus ground based detection methods can provide only a limited spatial array of information.

Remote Sensing Techniques

Volcanic activity can also be detected using a number of different remote sensing techniques. Some important geophysical features which can be observed using remote sensing are ground deformations, sulphur dioxide emissions, and gravity, magnetic and thermal anomalies. The main advantages of remote sensing are the high spatial density of data, and relatively low cost. On the other hand, these techniques are usually hindered by low temporal resolution, and often there are time delays between the acquisition and processing of data. These techniques can also require complex data processing, which can further delay the process. Therefore remote sensing techniques are often incapable of providing early warnings for volcano eruptions, and can only be utilised for post eruption analysis.

Geodetic Techniques

There are a number of geodetic techniques that can provide useful information for monitoring volcanoes. These methods consist of both on-site surveying techniques, such as GPS, levelling and tiltmeters, and remote sensing techniques, such as satellite radar interferometry. These techniques are all used to measure deformations in the earth's surface, and from these deformations one can deduce changes in the magma body beneath the caldera. This report focuses on the use satellite radar interferometry, which is outlined in the following section.

INSAR

Interferometric synthetic aperture radar (InSAR) is a remote sensing technique for measuring changes in topography over time. The technique originated from the field of radio astronomy, before being adapted to Earth-based measurements (Goldstein et al., 1988; Gabriel et al. 1989). InSAR can be used to detect centimetre-scale vertical deformations at a horizontal resolution of tens of meters. The technique has become a common geodetic tool, used routinely to measure surface deformation associated with earthquakes and volcanic eruptions. There are extensive reviews of the InSAR technique available in the literature (Massonnet and Feigl, 1998; Rosen et al. 2000; Zebker, 2000; Dzurisin, 2003; Richards, 2007). We give a brief outline of the steps involved in InSAR, followed by a discussion of its potential and limitations.

SAR Images

Synthetic aperture radar (SAR) is an imaging technique that uses a moving radar sensor to capture signals over a large area. SAR systems are generally mounted on aircraft or satellites. A SAR system emits a radar beam to the ground, with a known phase and frequency and constructs an image from the reflected beam using three measurements (Harger, 1970). These measurements are:

- Phase - corresponding to a time delay associated with the distance between the radar and the ground point
- Doppler shift - measuring the relative velocity between the radar system and the ground point
- Intensity - the reflectivity of the ground at each point.

Assuming the ground area of interest is flat, the phase and the Doppler signals can be used to uniquely determine the location of the signal in 2D space. Thus an image of intensity can be formed using the 2D coordinate system from the phase and Doppler signals (Harger, 1970).

While SAR can be used as a conventional imaging system, a more exciting application for geodesy is interferometric synthetic aperture radar (InSAR) where 2 or more SAR signals are combined to measure deformation of the surface. SAR systems operate by emitting and receiving a coherent, monochromatic radio beam. The radio beam is emitted at microwave frequencies, in one of the X, C, S, L or P bands (Elachi, 1988; Bamler and Hartl, 1998). The frequency and wavelength intervals of each of these bands are listed in Table 1 (Dawson, 2008).

Table 1: Frequencies and wavelengths of the microwave bands used in SAR acquisitions (Dawson, 2008).

BAND	FREQUENCY (GHZ)	WAVELENGTH (CM)
P	< 0.3	100
L	1-2	15-30
S	2-4	7.5-15
C	4-8	3.75-7.5
X	8-12	2.5-3.75

Topography

Since SAR images are formed in two dimensions only, the impact of topography must be taken into account when analysing the signal. Regions of elevated topography shorten the range between the satellite and the ground, which alters the phase signal. Therefore SAR images must be corrected for topography. This can be done using a reference digital elevation model (DEM), or by deducing a topographic phase signal from two SAR images (eg: Rosen et al. 2000). In order to measure topography from two different SAR images, the satellite tracks must measure the image from slightly different trajectories. The two signals differ slightly due to parallax, and these parallax differences can be inverted to solve for height at each point.

Interferometry

Once two SAR images have been acquired, the phase differences between the two images are used to measure line of sight deformations of the topography. The map of the phase differences is called an interferogram, where large deformation signals are represented by a series of periodic fringes in the phase. The process of forming an interferogram requires that the two phase maps are ‘coherent’, which means that the surface response between the two acquisitions remains similar. Coherence also requires that the two SAR images have been acquired from very similar look positions, otherwise parallax changes the apparent shape of the topography.

Figure 1 shows a schematic diagram of the geometry of InSAR. $\mathbf{A_1}$ and $\mathbf{A_2}$ represent the satellite positions, and ρ_1 and ρ_2 are the corresponding values of range from the satellite to the ground area being imaged. The unit vector in the direction from the satellite to the ground is known as the ‘look vector’. **B** is the ‘baseline’ vector, and represents the separation between the two satellite positions. $B_\perp$ is the ‘perpendicular baseline’, and represents the satellite separation in the direction perpendicular to the look vector.

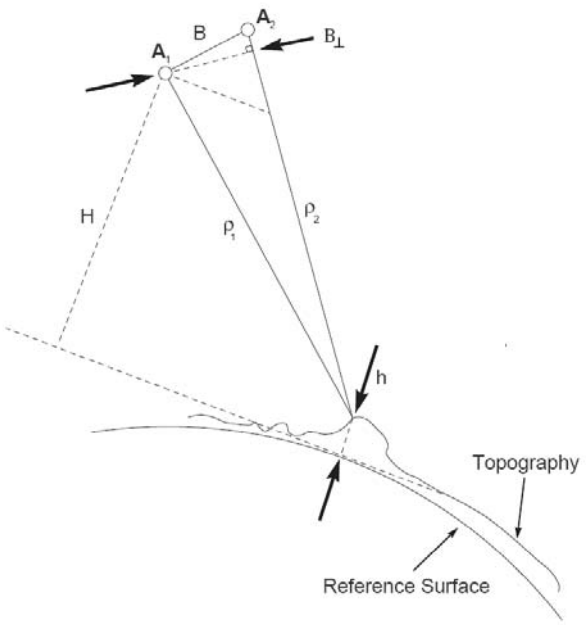

***Figure 1**: Schematic diagram of the geometry of InSAR, discussed in the text. Figure adapted from Bürgmann et al. (2000).*

When the two SAR images are compared, a change in range δρ between the images is deduced from the phase change δφ between the radar signals, using

$$\delta\rho = - \lambda / 4\pi * \delta\varphi,$$

where λ is the radar instrument wavelength. δρ can then be interpreted as a deformation of topography, in the line of sight of the satellite.

Phase Unwrapping

Phase is a periodic quantity, and cycles over the interval (-π,π]. Phase values larger than π, or smaller than –π are simply 'wrapped' back into the interval, by adding or subtracting a multiple of 2π. For example, a phase value of 3π is equivalent to π. The periodicity of the phase means that the range is initially ambiguous, as multiple values of range correspond to the same phase measurement.

In order to reconstruct the actual range map, the ambiguity of the phase must be removed through a process called 'unwrapping'. Phase unwrapping assumes that the phase changes (from the real signal) between neighbouring pixels are small compared to the 2π interval in which the signal is wrapped. If this assumption holds, then large phase differences (comparable to 2π) between pixels can be identified as periodic phase jumps and corrected by adding or subtracting 2π. A further requirement of the unwrapping process is that the sampling interval must be below a critical threshold, so that neighbouring pixels are close enough to each other to ensure that the phase map is smooth. In regions of steep topography, for example around cliffs, the unwrapping process breaks down, since it cannot distinguish between unwrapping errors and naturally large phase changes.

Limitations of InSAR

Different factors can hinder the acquisition and processing of InSAR data. One of the main difficulties is that the surface backscatter response must remain consistent between SAR acquisitions. This consistency is needed, because the phase signal must be coherent to form an interferogram between SAR images. If the land is reshaped by processes such as erosion or heavy precipitation, it can become impossible to form a coherent interferogram. Radar phase measurements can also be altered by atmospheric features, such as water vapour or interference from the ionosphere. This atmospheric noise means that the InSAR technique is generally more reliable if a large number of SAR acquisitions are available. When a long time series is available, the atmospheric signal can be reduced using temporal filtering (Berardino et al., 2002).

These issues can limit the capacity of InSAR to be used as an early warning system for volcano eruptions. Sometimes the deformation signal from a recent SAR acquisition cannot be reliably analysed until several later acquisitions have been taken. Since repeat pass times are of the order of 1 month, the time delay between the actual deformation event and the completion of data processing may be several months. It is for this reason that most InSAR studies of volcanoes have been conducted after the event, as opposed to using InSAR as a real-time monitoring system.

The choice of radar wavelength also places limitations on the operational capacity of InSAR. Shorter wavelengths, such as C-band and X-band, can provide higher precision measurements. However, these shorter wavelengths cannot penetrate vegetation. On the other hand, L-band radar can generally penetrate vegetation, so it is generally reflected by the ground itself. Thus in order to achieve global InSAR coverage from a single satellite mission, L-band wavelengths are the most reliable, even though they do not provide the highest precision (Stevens and Wadge, 2004).

The use of SAR imagery in creating topographic maps creates a minor conflict of interest for InSAR data acquisition. When measuring topography using InSAR, it is advantageous to have a larger baseline between data acquisitions. This is because a larger baseline creates a greater parallax signal, which increases the precision of topography measurements. On the other hand, forming an interferogram between SAR images requires a small baseline between acquisitions to achieve coherence between the two phase maps (Rosen et al., 2000). Therefore a SAR mission cannot be optimised for both topographic mapping and measurement of deformation. Since there are a limited number of satellites that acquire SAR data, these conflicting needs can reduce the data available for InSAR.

Data

ALOS PALSAR ACQUISITIONS

The SAR images used in this study were acquired by the ALOS PALSAR satellite, operated by the Japan Aerospace Exploration Agency (JAXA). A total of 10 images, between the dates of 12 January 2007 and 17 January 2009 were obtained from JAXA. On the JAXA online catalogue, these images can be located using its observation number: 352, and its scene ID: 7090. The image acquisition dates are shown in Table 2. Seven of the ten images formed a small baseline subset, and were used to form a series of interferograms. Unfortunately, 3 of the images had large orbital separations from the small baseline subset, which made them unsuitable for forming interferograms. This limited the time series to between the dates of 27 February 2007 and 16 April 2008, as indicated in Table 2.

Table 2: Dates of SAR images acquired for this study. Images 2-8 all had relatively short baselines with respect to each other. This subset of images 2 to 8 will be referred to as the small baseline subset, since the baseline values were of the order of 200 m. Images 1, 9 and 10 had much larger separations (approximately 1000 m) from the small baseline subset, which made it impossible to form interferograms with these images.

IMAGE #	IMAGE DATE	SUITABLE FOR INTERFEROGRAMS?
1	12 January 2007	no
2	27 February 2007	yes
3	15 July 2007	yes
4	30 August 2007	yes
5	15 October 2007	yes
6	15 January 2008	yes
7	01 March 2008	yes
8	16 April 2008	yes
9	17 October 2008	no
10	17 January 2009	no

INTERFEROGRAM PROCESSING

The 7 SAR images from the small baseline subset were processed to create a series of 19 interferogram pairs. These interferogram pairs are listed in Table 3, showing the dates of the images, and their perpendicular baselines. As discussed in the introduction, interferograms can only be formed if the baseline is relatively small. Each interferogram pair consists of a 'master' and a 'slave' image, where the master image is assigned to the later date by convention. Thus the master image can be interpreted as a deformation with respect to the slave image.

The interferograms were processed using the Repeat Orbit Interferometry Package (ROI-PAC). ROI-PAC is an open source software package, provided by the Jet Propulsion Laboratory of the National Aeronautics and Space Administration (NASA).

Table 3: List of the 19 interferogram pairs formed for this study, showing the dates of the SAR images, the perpendicular baseline, and the time between images. The interferogram pairs are grouped below according to the 6 different master image dates.

INTERFEROGRAM #	MASTER IMAGE DATE	SLAVE IMAGE DATE	PERPENDICULAR BASELINE (M)	ΔT (DAYS)
1	15 July 2007	27 February 2007	32	138
2	30 August 2007	27 February 2007	143	184
3	30 August 2007	15 July 2007	111	46
4	15 October 2007	27 February 2007	171	230
5	15 October 2007	15 July 2007	139	92
6	15 October 2007	30 August 2007	28	46
7	15 January 2008	15 July 2007	129	184
8	15 January 2008	30 August 2007	228	138
9	15 January 2008	15 October 2007	248	92
10	01 March 2008	27 February 2007	215	368
11	01 March 2008	15 July 2007	230	230
12	01 March 2008	30 August 2007	329	184
13	01 March 2008	15 October 2007	349	138
14	01 March 2008	15 January 2008	101	46
15	16 April 2008	15 July 2007	237	276
16	16 April 2008	30 August 2007	336	230
17	16 April 2008	15 October 2007	356	184
18	16 April 2008	15 January 2008	108	92
19	16 April 2008	01 March 2008	7	47

A major challenge in the processing of interferograms is to obtain coherence between the phase maps of different SAR images. To achieve coherence between SAR images, it usually necessary to apply spatial averaging to reduce noise. The standard spatial averaging method used in InSAR is 'multilooking'. This consists of grouping neighbouring pixels into blocks, and generating a new pixel from the average value of the block. As well as reducing noise, this technique allows the image to be resampled into square pixels (as the raw data consists of rectangular pixels). The drawback of multilooking is that it reduces the resolution of the interferogram. Therefore it is advantageous to set the multilook interval to the lowest possible value that will produce a coherent interferogram. In this study, each pixel was multilooked using 8 pixels in the range direction. (We also attempted to use a multilook interval of 4 range pixels, however this caused many of the interferograms to become incoherent.) The azimuth multilooking ratio was adjusted relative to achieve the same pixel length as the range direction.

INTERFEROGRAM STACKING

The interferograms described above measure the deformation between pairs of SAR images only. The next stage of the analysis was to stack the interferograms together, to form a time series of deformations over the entire period of data acquisitions. Since all of the interferograms used in this study come from the same small baseline subset, the stacking process consisted of a simple least squares solution. If the interferograms did not form a single baseline subset, the stacking process would be more complex. A full description of the stacking algorithm used to create this least squares solution is given by Berardino et al. (2002).

Results

SINGLE INTERFEROGRAMS

The SAR images used in this study cover a large area in the north-east of New Britain. Figure 2 shows a sample interferogram, which shows the full extent of the SAR images (in colour), with topography overlaid on the image. The area of interest around Rabaul is much smaller than this image, so for the remainder of the analysis, we restrict our field of view to the Rabaul area only.

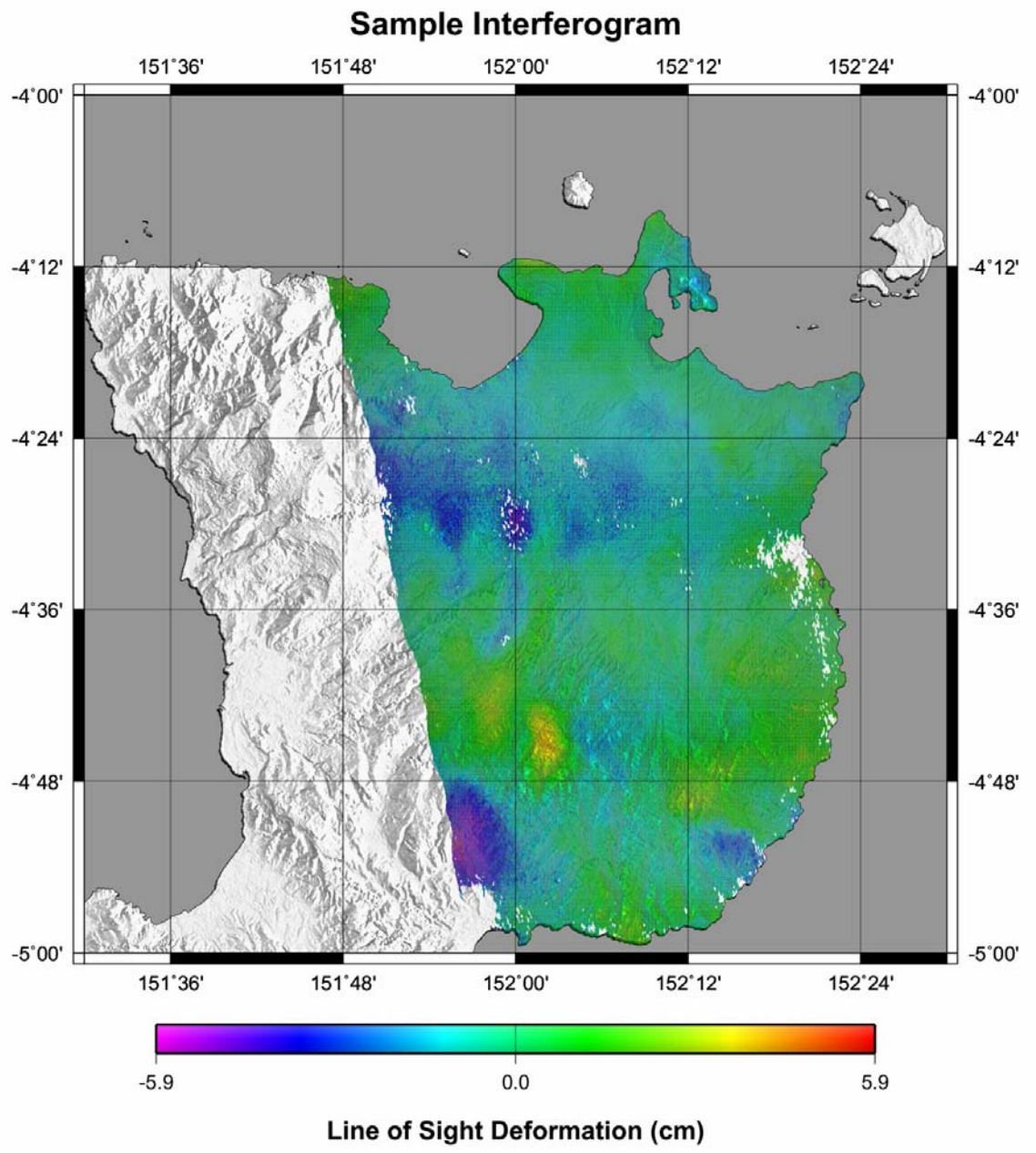

Figure 2: *A sample interferogram, showing the full extent of the image swath, as well as the topography in the north-eastern region of New Britain.*

The 19 pairs of interferograms formed in this study were subject to differing levels of coherence. In most cases, a shorter baseline and temporal separation lead to greater coherence. An example of this is shown by comparing Figure 3a with 3b, showing interferograms of high and low coherence respectively. The baseline and temporal separations in Figure 3a are much smaller than those in Figure 3b.

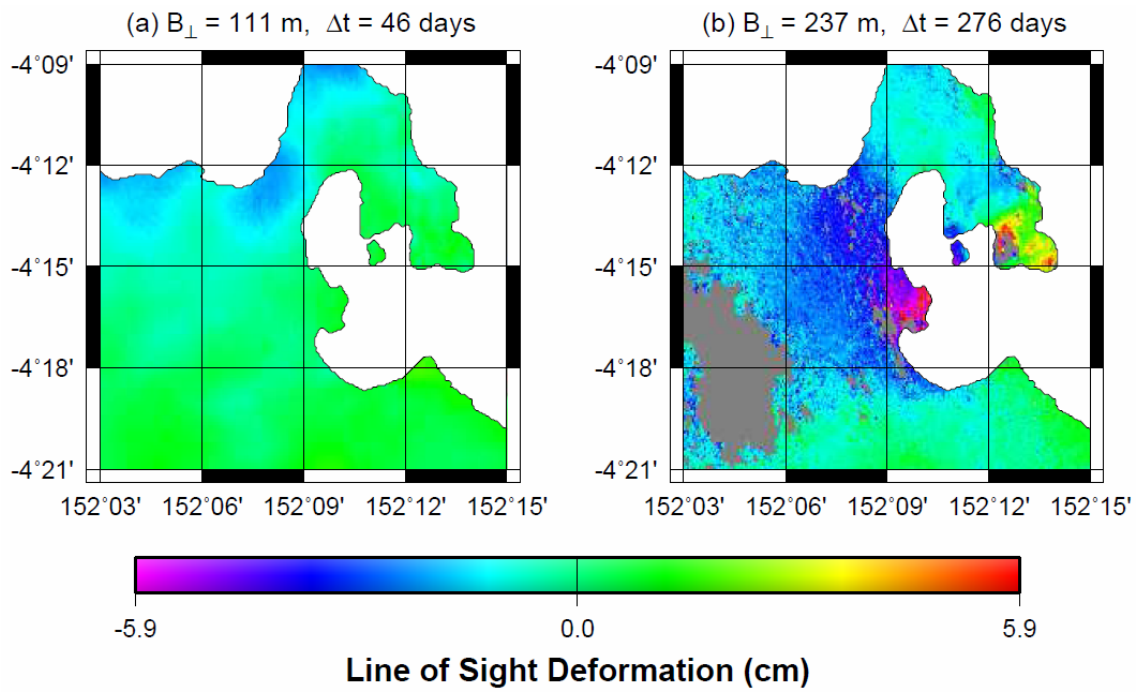

Figure 3: *A sample showing the differing coherence levels in the interferograms created. (a) shows a highly coherent interferogram, with a short baseline and temporal separation. (b) shows an interferogram with lower coherence, with a longer baseline and temporal separation. The grey areas in (b) represent pixels that have fallen below a coherence threshold of 0.1.*

TIME SERIES OF DEFORMATIONS

The interferograms were stacked together to form a time series of deformations, using the algorithm of Berardino et al. (2002). Some pixels fell below the coherence threshold, like those shown in Figure 3b, and so were assigned no value in the single interferogram processing. In order to run the stacking algorithm, these missing pixels were assigned values using nearest-neighbour interpolation.

The steps in the time series corresponded to the 7 dates of the SAR images. The first date (27-02-2007) in the series was assigned a deformation value of zero, and the subsequent 6 dates were measured as deformations with respect to the first date. These deformations are shown in the series of images in Figure 4. The series shows little change in the first two images (Figures 4a-b), apart from a small area of subsidence to the south-west of Tavurvur.

Figures 4c-f show broad subsidence around the Kombiu volcano, to the north-east of Tavurvur. These time steps also show the beginning of subsidence around Vulcan. Both of these signals are evident in 4 successive images. It is therefore likely that these two areas of subsidence are real signals, as an atmospheric artefact is unlikely to persist through multiple time steps. However, the amplitude (~ 5 cm) and spatial extent of the subsidence around Vulcan is significantly larger in the final time step (Figure 4f) than in the previous ones. It would therefore be desirable to extend the

time series past this final step, to exclude the possibility that the Vulcan subsidence is due to atmospheric noise. It would also be useful to corroborate this signal against ground-based GPS measurements.

Figure 4e shows large amplitude signals (~ 8 cm) of subsidence that are not present in either the previous or next time steps. It is possible that this signal of subsidence may be partly due to atmospheric noise. If the signal is real, it implies a trend of broad subsidence over a 46 day period, followed by an opposite trend of uplift of similar magnitude over the following 47 day period. While it is possible for deformations such as these to occur over short timescales, the immediate reversal of the subsidence suggests that atmospheric noise may be a factor. Without further data to corroborate this signal, it is difficult to distinguish between the possible atmospheric and geodetic contributions.

The subsidence in the Kombiu region is a very consistent trend in the time series. In addition to the longer term trend, the strong subsidence apparent in Figure 4e also occurs close to this region, though in this time step atmospheric noise may be a factor (as discussed above). This Kombiu subsidence coincides with a low-velocity anomaly found using seismic tomography (Bai and Greenhalgh, 2005). This low-velocity anomaly may be evidence of a magma chamber, making the Kombiu area one of volcanological interest. Although the time series in this study is somewhat sparse, the subsidence found suggests that further geodetic monitoring of Kombiu may be of interest.

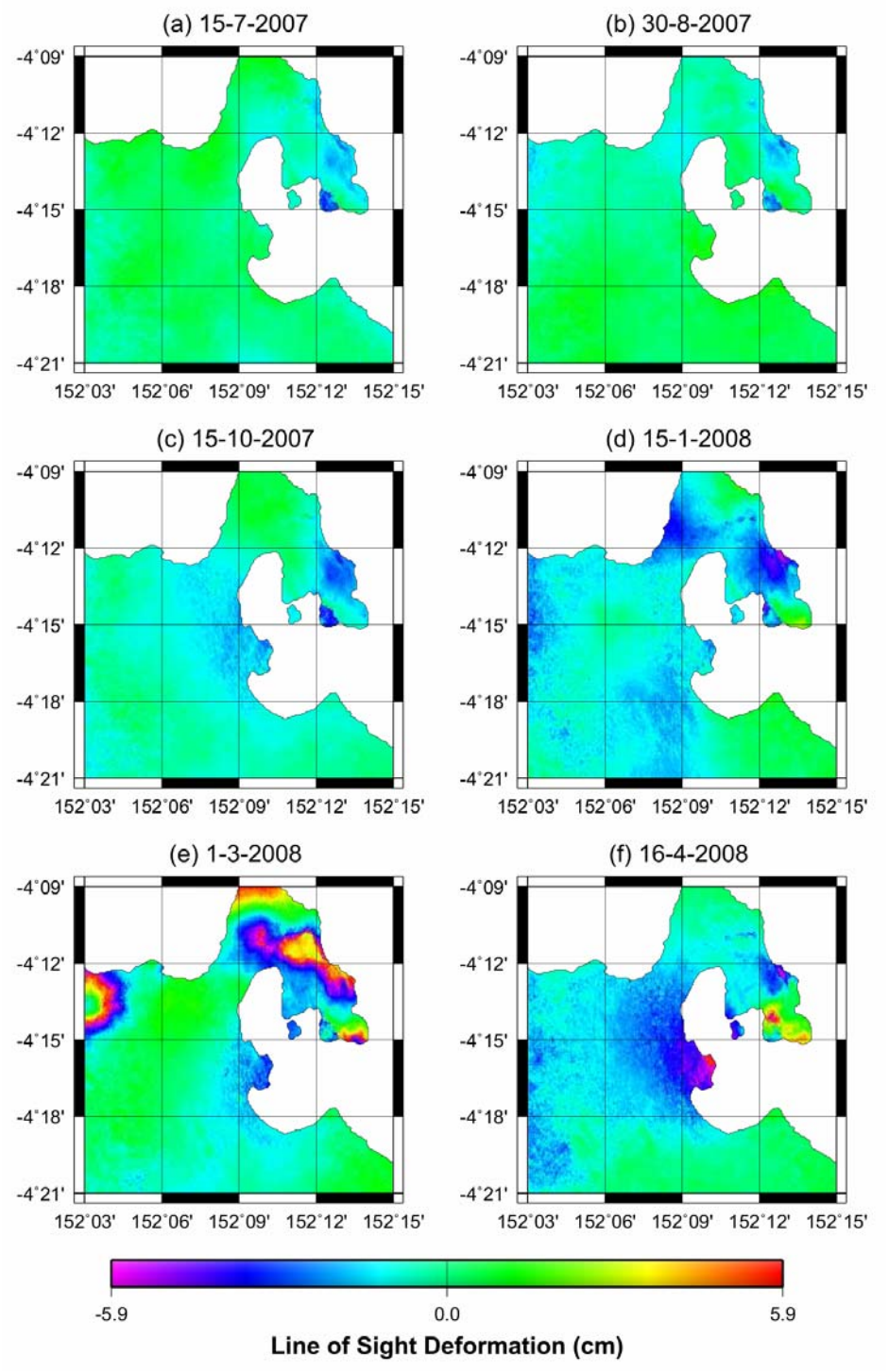

Figure 4: *Deformations shown at each time step, using the stacking method of Berardino et al. (2002). The deformations are measured with respect to the first SAR image, taken on 27-02-2007.*

The RVO has three GPS stations in the area, which in principle can be used to ground-truth the deformation signals found in this InSAR study. However, only one of the GPS stations was

operational during the time period of this study. This station was located on Matupit Island. Figure 5 shows a time series of deformations, comparing the GPS data from the RVO (RVO, 2009) with the InSAR deformation signal from the same location. The deformation signal shows a reasonable agreement for most of the time series, although the GPS data shows a trend of subsidence (up to 6 cm) at the end of the time series that is not matched by the InSAR data (roughly 2-3 cm). It would be therefore of interest to extend the InSAR time series (if the data were available), to see if this trend of subsidence is seen in further time steps.

It should also be noted that Matupit Island is not an ideal location for interferogram processing, since it is a very small area of land surrounded by water. Small islands like this are prone to unwrapping errors. The unwrapping process is usually more reliable when performed over large, contiguous areas of land.

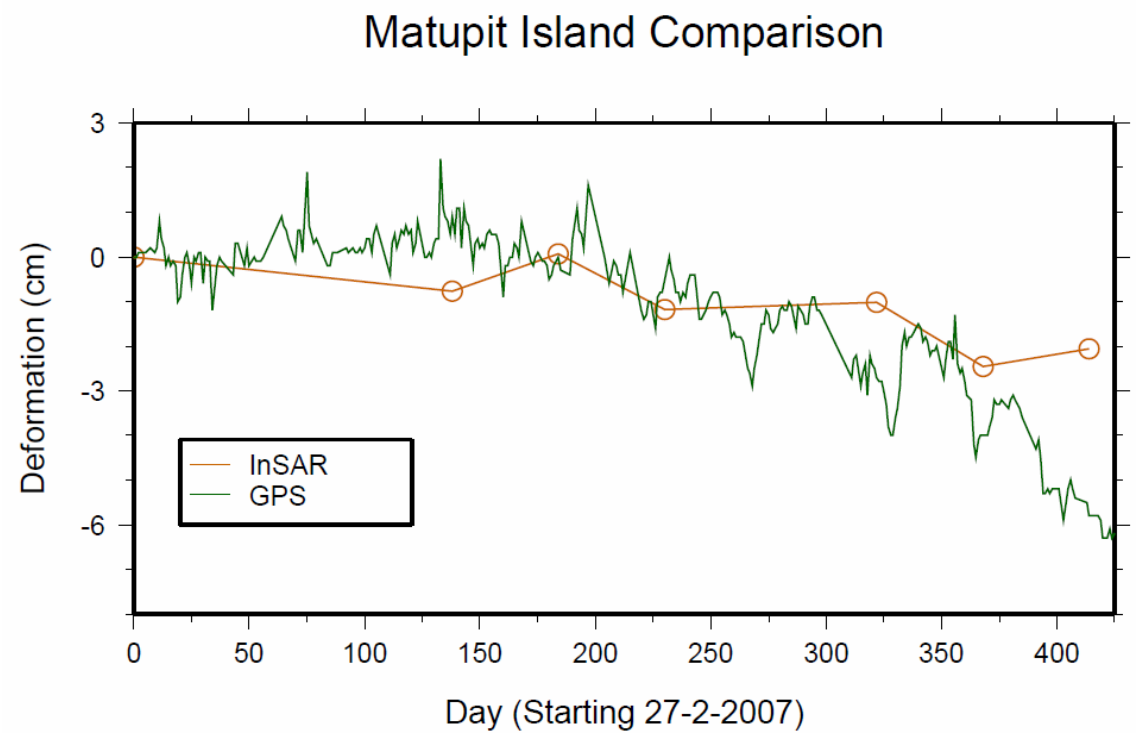

Figure 5: *Time series of deformations at Matupit Island, comparing the GPS data from the RVO, with our InSAR results from the same location.*

Discussion

This study has demonstrated the potential of InSAR to be used as a monitoring tool for volcanoes in PNG. The ALOS L-band radar acquisitions have been successfully processed to form a time series of deformations, spanning a 14 month period. Seven of the 10 SAR images purchased for this area formed a short baseline subset, suitable for interferogram processing. The primary limitation to the time series was the availability of data. Only 10 images were available over this area within a period of 2 years. This forced us to form interferograms with large temporal separations (some larger than 6 months). A greater frequency of SAR images would also allow us to apply temporal filtering, to remove atmospheric errors.

Rabaul was chosen as the location of this pilot study because there are independent data available to validate the results. It is now possible to compare the deformation signals found here with ground based measurements of deformations collected by the RVO. Drawing comparisons with the ground based data will be an important step in assessing the accuracy of InSAR in PNG. In the long term, InSAR promises to be especially useful in areas where ground based measurements are not available. Using the global coverage of SAR satellites, InSAR can be used to monitor any of the numerous volcanoes in PNG, and the region.

In terms of providing volcano warnings, ground based measurements will always be necessary, since they are needed to record geophysical change in real time. However, these ground based instruments cannot be installed everywhere, since they are costly and require on-site maintenance. Therefore ground based monitoring systems are generally placed only in locations where volcanoes are known to be hazardous. InSAR could be used to identify volcanoes that are becoming active. This information could then be used to select locations where better real time monitoring systems are needed.

Conclusion

ALOS SAR images were processed to form an array of interferograms. These interferograms were stacked together to form a time series of deformations, spanning a 14 month period from 27-2-2007 to 16-4-2008. A broad region of subsidence was found around Vulcan and Kombiu, although the amplitude of deformation was only about 6 cm in both cases. The centimetre-scale precision, and relatively low noise in the interferograms suggest that this technique could feasibly detect uplift or subsidence as precursors to an eruption. InSAR therefore has the potential to identify volcano hazards, which will be especially useful in the absence of ground based monitoring systems.

ACKNOWLEDGEMENTS

We would like to thank Steve Saunders and Ima Itikarai from the RVO, for providing us with useful information from their ground based observations, including GPS and tiltmeter data. We would also like to thank Shane Nancarrow and Wally Johnson for their advice and feedback during the project.

REFERENCES

AusAID, 1996. *Papua New Guinea – Australia Volcanological Service Support Project Phase 2*. Project Design Document: Australian Agency for International Development.

Bamler, R. and Hartl, P., 1998. Synthetic aperture radar interferometry. *Inverse Problems,* **14(4)**: 1.

Berardino, P., Fornaro, G., Lanari, R., and Sansosti, E., 2002. A new algorithm for surface deformation monitoring based on small baseline differential SAR interferograms. *IEEE Trans. Geosci. Remote Sens.,,* **40(11)**: 2375-2383.

Bürgmann, R., Rosen, P. and Fielding, E., 2000. Synthetic aperture radar interferometry to measure Earth's surface topography and its deformation. *Ann. Rev. Earth Planet Sci.* **28**: 169-209.

Dawson, J., 2008. *Satellite Radar Interferometry with Application to the Observation of Surface Deformation in Australia.* Ph.D. thesis, The Australian National University.

Dzurisin, D., 2003. A comprehensive approach to monitoring volcano deformation as a window on the eruption cycle. *Rev. Geophys.,* **41(1)**: 1001.

Elachi, C., 1988. *Spaceborne radar remote sensing.*IEEE-Press.

Fisher, A., 2005. Volcano Monitoring in the Asia-Pacific Region with Satellite Imagery. *Internal report,* Geoscience Australia.

Finlayson, D., Gudmundsson, O., Itikarai, I., Nishimura, Y., and Shimamura, H., 2003. Rabaul volcano, Papua New Guinea: seismic tomographic imaging of an active caldera. *Journal of Volcanology and Geothermal Research,* **124**: 153-171.

Gabriel, A., Goldstein, R., and Zebker, H., 1989. Mapping small elevation changes over large areas: Differential radar interferometry. *J. Geophys. Res.,* **94(B7)**: 9183-9191.

Goldstein, R., Zebker, H., and Werner, C., 1988. Satellite radar interferometry: two-dimensional phase unwrapping. *Radio Sci.,* **23(4)**: 713-720.

Harger, R., 1970. *Synthetic Aperture Radar Systems: Theory and Design.* Academic Press.

Massonnet, D. and Feigl, K., 1998. Radar interferometry and its application to changes in the earth's surface. *Rev. Geophys.,* **36(4)**: 441-500.

Richards, M., 2007. A beginner's guide to interferometric SAR concepts and signal processing. *IEEE Aerospace and Electronic Systems Magazine,* **22(9)**: 5.

Rosen, P., Hensley, S., Joughin, I., Li, F., Madsen, S., Rodriguez, E., and Goldstein, R., 2000. Synthetic aperture radar interferometry. *Proc. IEEE,* **88(3)**: 333-382.

RVO, 2009. Personal communication of unpublished GPS data.

Stevens, N. and Wadge, G., 2004. Towards operational repeat-pass SAR interferometry at active volcanoes. *Natural Hazards,* **33(1)**: 47-76.

Zebker, H., 2000. Studying the Earth with interferometric radar. *Computing in Sci. & Eng.,* **2(3)**: 52-60.